JOURNAL OF THERMOPHYSICS AND HEAT TRANSFER
Vol. 12, No. 3, July–September 1998

Parametric Study of Actively Cooled Aircraft Structure

S. C. Griggs*
Lockheed Martin Corporation, Fort Worth, Texas 76101
and
A. Haji-Sheikh†
University of Texas at Arlington, Arlington, Texas 76019-0023

Embedded cooling channels in the skin is one method of protecting high-speed air vehicles from high-temperature environments. A closed-form solution is used to predict temperature and heat flux in a material layer with embedded cooling channels. A solution of the energy equation predicts the localized and global effects of temperature in the material and embedded cooling channels. Two parametric studies were conducted: one considers the composite material to be homogeneous and the other considers the material orthotropic. The analytical solution is an integral method that uses the Green's function to conduct a parametric study of embedded cooling channels in a composite aircraft skin.

Nomenclature

A = matrix
a, b = geometric dimensions
a_{ij} = elements of matrix A
B = matrix
Bi = Biot number, hb/k_{my}
b_{ij} = elements of matrix B
c = radius of a flow channel
c_p = specific heat, J/kg K
D = tube diameter, m
$\boldsymbol{d}_n$ = eigenvectors with elements d_{nj}
d_{nj} = coefficients
f_j = basis function
g = volumetric heat generation, W/m^3
H = auxiliary function
h = heat transfer coefficient, W/m^2 K
k = thermal conductivity, W/m K
N = number of eigenvalues
Nu = Nusselt number, h_eD/k_e
$\boldsymbol{n}$ = unit vector
P = inverse of the transpose of DB matrix
p_{ni} = elements of matrix P
q = heat flux, W/m^2
$\boldsymbol{r}$ = position vector, in xy coordinates
$\boldsymbol{r}'$ = position vector, dummy variable
S = surface
T = temperature, °C
T^* = auxiliary or quasisteady temperature, °C
u = velocity, m/s
V = volume, m^3
x, y, z = coordinates
z' = axial flow position vector, dummy variable
γ_n = eigenvalue
μ = viscosity coefficient, N/s m^2
ρ = density, kg/m^3
ϕ = boundary function
ψ_n = orthogonal function
Ω_m = function, Eq. (15)

Subscripts
av = average quantity
e = inclusion (fluid)
i = inside wall condition
ins = insulation
m = main domain
n, p = indices
o = outer wall condition
s = at surface
x, y, z = direction of x, y, z axes
∞ = ambient condition

Introduction

SKIN temperature control is important to the aerospace industry for high-speed air vehicles, thermal laminar flow control on supersonic civil transports, or infrared signal suppression on military vehicles. This necessitates a study of temperature and heat flux to protect advanced composite-material skins. A cooling system for these applications may consist of multiple cooling channels placed in the skin to provide uniform cooling.

Composite materials have been of interest to the aerospace industry because of their light weight and increased durability at high temperatures. The structural and thermal communities have characterized composite materials to predict stress and strain and to predict temperature and heat flux, respectively. The increased use of composites in high-temperature applications requires temperature-prediction capabilities to ensure part integrity and thermal protection of the surrounding structure. Cooling of composite laminate skins on air vehicles can be accomplished by utilizing cooling channels embedded in the skins. Cooling channels can create high thermal gradients in a composite laminate whenever a high heat flux is present. Testing methods for parametric studies and temperature prediction in composite laminates are expensive. Moreover, the calculation of heat flux from the measured temperature data requires a significant numerical effort. Therefore, mathematical and numerical methods can be utilized to predict temperature profiles and local heat flux in the composite material and the cooling channel fluid.

Finite difference and finite element techniques have been the mathematical and numerical methodologies most prevalent in the aerospace industry for the last three decades. These temperature-prediction techniques use a lumped-parameter meth-

Received Nov. 21, 1997; revision received March 10, 1998; accepted for publication March 11, 1998. Copyright © 1998 by the American Institute of Aeronautics and Astronautics, Inc. All rights reserved.

*Specialist Senior, Power, Thermal, and Propulsion Systems, P.O. Box 748.

†Professor, Department of Mechanical and Aerospace Engineering. Senior Member AIAA.

odology to discretize a global domain into many subdomains. Solution techniques utilized in finite element and finite difference analyses depend upon whether elliptic, parabolic, or hyperbolic partial differential equations are being solved.[1] The main objective of this paper is to accurately calculate the heat flux from composite lamina to the coolant; therefore, it is desirable to satisfy continuity of temperature and heat flux everywhere along the boundary of cooling channels. An integral method, used to accomplish this task, is a subset of the p-type finite element method with spectral characteristics. All numerical steps in this integral method are based on the method of weighted residuals. This method provides a continuous temperature and heat flux distribution in all domains of interest. This is beneficial when calculating heat flux and, in particular, the computation of the Nusselt number in the flow channels. Another benefit for utilizing integral methods is that symbolic mathematical software can be used to conduct all integration and matrix algebra. This allows the configuration design parameters to be considered as undefined constants throughout the calculation process. The temperature profile is then available as a function of changing design parameters.

This integral method leads to a Green's function method that simultaneously solves the energy equation in the lamina and flow channels. By properly defining the basis functions, one can accommodate boundary conditions of the first, second, or third kind on each boundary surface and, in addition, the conservation of heat flux and continuity of temperature all along the interface between the lamina and the coolant. The Green's function solution simultaneously leads to relations for the temperature profile in the cooling channels and the temperature profile in the laminate.

First, this analytical solution is validated. It is assumed that a convective boundary condition exists at both surfaces as they are exposed to a high-temperature environment. For simplicity, the sample problem analyzes a single cooling channel's domain. This simulates equally spaced cooling channels embedded in a lamina while adiabatic boundaries are located at the midpoint between adjacent cooling channels. However, the method equally applies to unequally spaced cooling channels with nonsymmetric convective boundary conditions. A brief description of the method of calculating temperature is in a separate section.

Following the validation, this solution technique is employed to conduct a parametric study of cooling channel spacing effects on the Nusselt number. Cooling channels are embedded in a composite material to remove heat from a hot surface of lamina, thereby reducing the temperature of the composite material to within design limits. Conducting parametric studies of this type allows for flexibility in the manufacturing of the aircraft skin and optimizing the fuel use for cooling the aircraft skin. The Green's function solution permits many configurations to be evaluated in a relatively short time frame. The component material properties and coolant material properties can be changed with ease.

Mathematical Formulation

Green's function solutions of the heat conduction equation for various shapes have been documented by Beck et al.[2] and Cotta.[3] The simultaneous solution to localized and global temperatures in embedded cooling channels requires an analytical technique to calculate temperature in nonorthogonal bodies with nonhomogeneous boundary conditions. Relevant reported investigations are in Refs. 4 and 5 and an overview of the solution method is in Ref. 2. A detailed discussion of the Galerkin method as a mathematical tool for solving boundary value problems is in Ref. 6.

Energy Equation

The objective is to provide a methodology for solving the energy equation in the flow and adjacent walls. The steady-state energy equation, in the generalized form, for both domains is

$$\nabla \cdot [k(\boldsymbol{r})\nabla T] + g = \rho(\boldsymbol{r})c_p(\boldsymbol{r})u(\boldsymbol{r})\frac{\partial T}{\partial z} \tag{1a}$$

where $T = T(\boldsymbol{r}, z)$ is temperature, $\boldsymbol{r}$ is the position vector, z is the axial flow direction, u is the flow velocity, and $g = g(\boldsymbol{r}, z)$ is the volumetric heat source. The thermophysical properties are density $\rho(\boldsymbol{r})$, specific heat $c_p(\boldsymbol{r})$, and thermal conductivity $k(\boldsymbol{r})$. Because $T(\boldsymbol{r}, z)$ describes the temperature in the fluid and the solid wall, the variables $\rho(\boldsymbol{r})$, $c_p(\boldsymbol{r})$, $k(\boldsymbol{r})$, and $u(\boldsymbol{r})$ are position dependent. The thermal conductivity $k(\boldsymbol{r})$, may also depend on direction. For orthotropic materials, the first term on the left-hand side of Eq. (1) is

$$\nabla \cdot [k(\boldsymbol{r})\nabla T(\boldsymbol{r}, z)] = k_{xx}\frac{\partial^2 T}{\partial x^2} + k_{yy}\frac{\partial^2 T}{\partial y^2} + k_{zz}\frac{\partial^2 T}{\partial z^2} \tag{1b}$$

where k_{xx}, k_{yy}, and k_{zz} are thermal conductivity values in the x, y, and z directions, respectively.

The following studies are for two different fiber arrangements in the composite skins. Figure 1a considers the fibers parallel to the flow direction; hence, the effective thermal conductivity is uniform in the xy plane. In Fig. 1b, the fibers are normal to the flow direction; therefore, the composite is orthotropic in the xy plane. Equation (1) describes temperature distribution for the two configurations shown in Fig. 1. Equation (1) is similar to the transient heat conduction in solids except $\partial T(\boldsymbol{r}, t)/\partial t$ is replaced by $\partial T(\boldsymbol{r}, z)/\partial z$ and $\rho(\boldsymbol{r})c_p(\boldsymbol{r})$ is replaced by $\rho(\boldsymbol{r})c_p(\boldsymbol{r})u(\boldsymbol{r})$. This energy equation governs the temperature field in fully developed steady-state fluid flow in a duct and its surrounding materials. Within the solid wall, $u(\boldsymbol{r}) = 0$, Eq. (1) reduces to the Poisson equation. The generalized boundary conditions for this study are $\partial T/\partial x = 0$ at $x = \pm a$, $-k\partial T/\partial y = h_o(T - T_s)$ at the outer surface, where $y = b$ and $-k\partial T/\partial y = q_i$ at the inner surface, where $y = -b$. The contact conditions between the solid wall require that the temperature and heat flux be continuous at $x^2 + y^2 = c^2$ surface.

Solution

For convenience of analysis, the solution of Eq. (1) is decomposed into two solutions

$$T(\boldsymbol{r}, z) = T^*(\boldsymbol{r}, z) + T_z(\boldsymbol{r}, z) \tag{2}$$

where $T^*(\boldsymbol{r}, z)$ is a differentiable auxiliary function that satisfies the nonhomogeneous boundary conditions similar to those for $T(\boldsymbol{r}, z)$. The function $T^*(\boldsymbol{r}, z)$ may be chosen arbitrarily or taken from the quasi-steady-state solution that satisfies the equation

$$\nabla \cdot [k(\boldsymbol{r})\nabla T^*(\boldsymbol{r}, z)] = 0 \tag{3}$$

Selection of a function $T^*(\boldsymbol{r}, z)$ that satisfies Eq. (3) will simplify the subsequent algebraic analysis. Then, the substitution of T from Eq. (2) into Eq. (1a) results in the equation

$$\nabla \cdot [k(\boldsymbol{r})\nabla T_z] + \bar{g} = \rho(\boldsymbol{r})c_p(\boldsymbol{r})u(\boldsymbol{r})\frac{\partial T_z}{\partial z} \tag{4}$$

The function $g = \bar{g}(\boldsymbol{r}, z)$ is the new volumetric heat source defined by the relation

$$\bar{g}(\boldsymbol{r}, z) = g(\boldsymbol{r}, z) - \rho(\boldsymbol{r})c_p(\boldsymbol{r})u(\boldsymbol{r})\frac{\partial T^*(\boldsymbol{r}, z)}{\partial z} \tag{5}$$

where $g(\boldsymbol{r}, z) = 0$ in the subsequent numerical calculations. The function $T_z = T_z(\boldsymbol{r}, z)$ remains to be determined for insertion in Eq. (2) and to obtain T. Function T_z must satisfy the

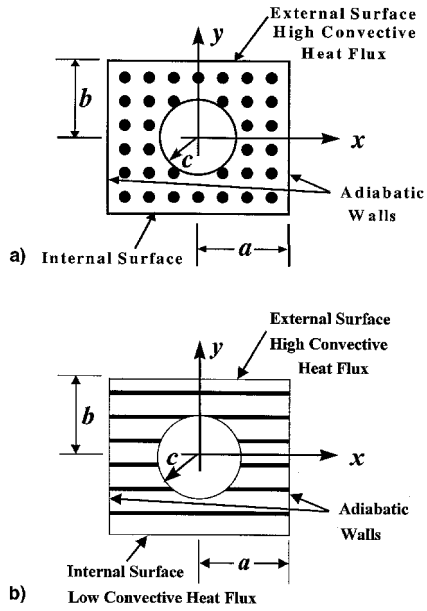

Fig. 1 Composite skin with cooling channels. Fibers a) parallel and b) perpendicular to the z direction.

homogeneous boundary conditions of the same type as the original problem. Following appropriate modifications and neglecting conduction in the z direction, $\boldsymbol{r}$ becomes the position vector in the xy plane, and the Green's function solution[2] for temperature, $T(\boldsymbol{r}, z)$, reduces to

$$T(\boldsymbol{r}, z) = T^*(\boldsymbol{r}, z) + \frac{1}{\rho(\boldsymbol{r})c_p(\boldsymbol{r})} \times \left\{ \int_{z'=0}^{z} dz' \int_A G(\boldsymbol{r}, z|\boldsymbol{r}', z')\bar{g}(\boldsymbol{r}', z')\, dx'\, dy' + \int_V \rho(\boldsymbol{r}')c_p(\boldsymbol{r}')u(\boldsymbol{r}')G(\boldsymbol{r}, z|\boldsymbol{r}', 0)[T(\boldsymbol{r}', 0) - T^*(\boldsymbol{r}', 0)]\, dx'\, dy' \right\} \tag{6}$$

This is an alternative form of the Green's function solution that has no singularities and properly converges in the vicinity of the external surfaces. The function, $G(\boldsymbol{r}, t|\boldsymbol{r}', z')$, is the Green's function, defined as

$$G(\boldsymbol{r}, z|\boldsymbol{r}', z') = \sum_{n=1}^{N} \rho(\boldsymbol{r}')c_p(\boldsymbol{r}')\psi_n(\boldsymbol{r})\bar{\psi}_n(\boldsymbol{r}')e^{-\gamma_n(z-z')} \tag{7}$$

The function $\psi_n(\boldsymbol{r})$ in Eq. (7) represents a set of orthogonal functions in the $\boldsymbol{r}$ domain. A proper selection of $\psi_n(\boldsymbol{r})$ is an essential part of this presentation. It is customary to define $\psi_n(\boldsymbol{r})$ as a linear combination of a set of basis functions as[2]

$$\psi_n(\boldsymbol{r}) = \sum_{j=1}^{N} d_{nj} f_j(\boldsymbol{r}) \tag{8a}$$

The function

$$\bar{\psi}_n(\boldsymbol{r}') = \sum_{i=1}^{N} p_{ni} f_i(\boldsymbol{r}') \tag{8b}$$

is related by orthogonality to $\psi_n(\boldsymbol{r})$. The method of selecting the basis functions and calculation of γ_n, d_{ni}, and p_{nj} is an important feature of this paper. The function $f_j(\boldsymbol{r})$ represents the basis function; i.e., a member of a set of linearly independent functions chosen so that the homogeneous boundary conditions are satisfied. The coefficients designated by d_{nj} are members of the eigenvector $\boldsymbol{d}_n$ of the equation

$$(A + \gamma_n B)\boldsymbol{d}_n = 0 \tag{9}$$

where A and B are matrices of size N with elements

$$a_{ij} = \int_V f_i(\boldsymbol{r})\nabla \cdot [k(\boldsymbol{r})\nabla f_j(\boldsymbol{r})]\, dx'\, dy' \tag{10}$$

$$b_{ij} = \int_V \rho(\boldsymbol{r})c_p(\boldsymbol{r})u(\boldsymbol{r})f_i(\boldsymbol{r})f_j(\boldsymbol{r})\, dx'\, dy' \tag{11}$$

The basis functions in Eqs. (10) and (11) are usually not orthogonal; therefore, matrices A and B have off-diagonal elements. The Jacobi method[7] is employed to compute the eigenvalues γ_n and eigenvectors $\boldsymbol{d}_n$ of Eq. (9). It can be shown that even if the basis functions are not orthogonal, the ψ_n are orthogonal. Matrix B is symmetric, $b_{ij} = b_{ji}$. Matrix A is also symmetric for homogeneous boundary conditions of the first, second, and third kind.[2] Once the eigenvectors and matrix B are available, the coefficients represented by p_{ni} are members of the matrix $P = [(D \cdot B)^T]^{-1}$, where D is a matrix whose rows are the eigenvectors.

Basis Functions

The difference between solutions for homogeneous and heterogeneous solids is the selection of a set of basis functions. For the solid material domain, a set of basis functions is defined that satisfies the boundary conditions on the external surfaces. For the channel flow, a different set of basis functions is defined that satisfies the continuity of temperature and heat flux at the boundary of the cooling channel. These basis functions are used in their respective domains for the calculation of elements of the matrices A and B.

Let the subscript e identify the cooling channel and let m denote the solid domain or main domain (Fig. 1). The basis function $f_{j,m}$, which satisfies the boundary conditions of the main domain, is selected ignoring the inclusion; therefore, f_j is $f_{j,m}$ in the main domain. However, the basis function should be modified as it crosses the boundary of the cooling channel. Assuming a cooling channel to be an inclusion and in the absence of contact conductance, the formulation of the basis function for the channel flow region follows the steps described in Ref. 8.

$$f_j = f_{j,m} \quad \text{(in the main domain)} \tag{12}$$

$$f_j = f_{j,e} = f_{j,m} + \phi_e H \quad \text{(in the } e\text{th inclusion)} \tag{13}$$

for $j = 1, 2, \ldots, N$. The continuity condition, that is, $k_m(\partial f/\partial n)_m = k_e(\partial f/\partial n)_e$ at the boundary of the inclusion permits the calculation of H for homogeneous materials

$$H = \frac{(k_m/k_e - 1)(\nabla f_{j,m} \cdot \nabla \phi_e)|_{\phi_e=0}}{(\nabla \phi_e \cdot \nabla \phi_e)|_{\phi_e=0}} \tag{14a}$$

When the material domain in the xy plane is orthotropic, the function H becomes

$$H = \frac{[\Omega_m - k_e(\nabla f_{j,m} \cdot \nabla \phi_e)]_{\phi_e=0}}{k_e(\nabla \phi_e \cdot \nabla \phi_e)|_{\phi_e=0}} \tag{14b}$$

where

$$\Omega_m = k_{mxx}\left(\frac{\partial f_{j,m}}{\partial x} \cdot \frac{\partial \phi_e}{\partial x}\right) + k_{myy}\left(\frac{\partial f_{j,m}}{\partial y} \cdot \frac{\partial \phi_e}{\partial y}\right) \tag{15}$$

The second derivative of function f_j is singular across the inclusion boundary. Rewriting Eq. (10) as[2]

$$a_{ij} = \int_V f_i \nabla \cdot (k \nabla f_j)\, dV$$

$$= \int_{V-V_e} f_{i,m} \nabla \cdot (k \nabla f_{j,m})\, dx'\, dy' + \int_{V_e} f_{i,e} \nabla \cdot (k \nabla f_{j,e})\, dx'\, dy' \tag{16}$$

alleviates this problem. Before attempting a parametric study, it is appropriate to validate this solution technique.

Mathematical Method Validation

Validation of the solution begins by studying a limiting case of a model shown in Fig. 1a. Both surfaces at $y = \pm b$ are subject to convective boundary conditions with equal heat transfer coefficients, $h = h_o = h_i$. As the heat transfer and thermal conductivity of the solid domain increases, the solution of this problem should approach the classical Graetz problem.

The basis functions describing the adiabatic boundary conditions at $x = \pm a$, Fig. 1, are

$$f_{x1} = \text{const} \tag{17a}$$

$$f_{xp} = \left(1 - \frac{x}{a}\right)^2 \left(1 + \frac{x}{a}\right)^p \quad \text{for} \quad p = 2, 3, 4, \ldots, N_p \tag{17b}$$

The basis functions in the y direction for convective boundary conditions are

$$f_{y1} = \left(\frac{2}{b} + \frac{2h}{k_{my}}\right)\left(\frac{y}{b}\right)^2 + 2\left(\frac{2}{b} + \frac{h}{k_{my}}\right)\left(-\frac{1}{b} - \frac{h}{k_{my}}\right) \tag{18}$$

$$f_{yn} = (b - y)^2 (b + y)^n \quad \text{for} \quad n = 2, 3, 4, \ldots, N_n \tag{19}$$

Although Eq. (19) does not contain a convection coefficient term (p. 269, Eq. 19 of Ref. 6), these basis functions have been employed for convective boundary conditions. Equations (18) and (19) do indeed satisfy the boundary conditions of the third kind, $-k_{myy}\partial f_j/\partial y = hf_j$ at $y = \pm b$. Accordingly, the $N = N_p N_n$ basis functions for the main domain are obtained using the relation $f_j = f_{xp} \times f_{yn}$, see Eqs. (17–19). For the channel flow domain, identified as the inclusion, Eq. (13) yields the basis functions $f_{j,e}$ after setting $\phi_e = x^2 + y^2 - c^2$.

Following the computation of matrices A and B, eigenfunctions, and eigenvalues, Eq. (6) provides the temperature distribution. Throughout this paper, it is assumed the diameter of flow passages is very small, the flow is laminar, and $u = 2u_{\text{av}}[1 - (x^2 + y^2)/c^2]$. Focusing attention on the flow in the passages, at any z location, the analytical values of the fluid bulk temperature T_{eb}, and the mean temperature of the tube wall $T_{s,\text{av}}$. The average convection coefficient $\bar{h}_e$ is defined as $\bar{h}_e = \bar{q}/(T_{s,\text{av}} - T_{eb})$, where $\bar{q}$ is the average heat flux at the wall, $T_{s,\text{av}}$ is the average wall temperature of the flow channels, and T_{eb} is the bulk channel flow temperature. The Nusselt number for flow in the channel is defined as $Nu_D = \bar{h}_e D/k_e$, where k_e is the thermal conductivity of the fluid in the channel. The energy balance on a fluid element in the flow channels yields $Nu_D = Re_D Pr(D/4)(dT_{eb}/dz)/(T_{s,\text{av}} - T_{eb})$, where $Pr = \mu_e c_{pe}/k_e$ is the Prandtl number and $Re_D = \rho u_{\text{av}} D/\mu_e$ is the Reynolds number. The fully developed Nusselt number is plotted as a function of k_m/k_e in Fig. 2; $k_m = k_{myy} = k_{mxx}$ is a shorthand notation because of the assumption of isotropy in the xy plane. It was observed that, in addition to the thermal conductivity ratio, the heat transfer coefficients over $y = \pm b$ surfaces influence the Nusselt number. Two sets of data using the Biot numbers, $Bi = hb/k_m$, of 0.1 and 1 are plotted in Fig. 2. For comparison, another set of data corresponding to a prescribed temperature at $y = \pm b$ is plotted in the same figure. For constant wall temperature ($h = \infty$) at $y = \pm b$, the basis functions

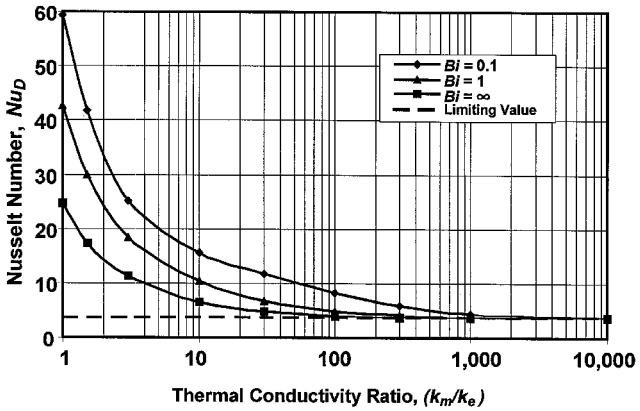

Fig. 2 Asymptotic behavior of the Nusselt number, $h_e D/k_e$, for solution validation.

$$f_{yn} = (b - y)(b + y)^n \quad \text{for} \quad n = 1, 2, 3, \ldots, N_n \tag{20}$$

are used instead of the functions given by Eqs. (18) and (19). The data show, as expected, that the asymptotic value of the Nusselt number[9] of 3.657, shown as a dotted line, is achieved at lower thermal conductivity ratios. Also, these results are used to verify the convergence of the solution. Solutions using 4 and 9 eigenvalues show little difference.

Results

Nine eigenvalues are employed for calculation of the temperature and heat flux requiring nine basis functions. The auxiliary function T^* for both sets of boundary conditions is set to 1093°C (2000°F). The global material thermal conductivity k_m and convection coefficient h are varied to set the global Biot number $Bi = hb/k_m$. The results of this study (Fig. 2), show that the methodology does agree with classical theory when the thermal conductivity of the global material is much greater than that of the fluid. Thus, by comparing the temperature and heat flux at large k_m/k_e values with theoretical results, the mathematical methodology has been validated, thereby installing confidence in this technique.

Parametric Study

This study consists of evaluating the heat transfer coefficient of cooling channels embedded in a carbon–carbon composite material. First, the mathematical process developed earlier is employed to calculate the Nusselt number in the thermal protection system for carbon–carbon composite skin shown in Fig. 1. The working fluid for this presentation is JP-8 jet fuel.

Configuration Definition

The fibers in a typical actively cooled air vehicle skin, constructed of composite materials with embedded cooling channels, are either parallel or perpendicular to the direction of flow, Figs. 1a and 1b, respectively. When the fibers are in the axial flow direction (Fig. 1a), the effective thermophysical properties in the xy plane are uniform. The orthotropic material properties are used for the carbon–carbon materials with the fibers layered perpendicular to the axial flow direction (Fig. 1b). The skin is exposed to a high-temperature convective environment on its external surface, $y = b$, and a low temperature convective environment on its internal surface, $y = -b$. Based on symmetry, it is assumed $q = 0$ at $x = \pm a$ and, as before, only one channel section is evaluated.

Basis Functions when $q = 0$ at $y = -b$

Basis functions must satisfy the homogeneous mathematical boundary conditions and not the nonhomogeneous boundary

conditions of the physical problem. The process of utilizing the mathematical methods for temperature determination requires careful selection of the basis functions as determined earlier.

It is essential for the temperature of the coolant to remain below a limit. For a conservative estimate of the coolant temperature, the first set of basis functions assumes insulated boundary, $q = 0$ at $y = -b$. This set of functions consists of a second-order polynomial multiplied by members of a complete set of functions. They were selected to satisfy the boundary conditions of the third kind[2] at $y = b$ and second kind at $y = -b$. The y contribution of the basis functions that satisfy boundary conditions of the third kind at $y = b$ and the second kind at $y = -b$ are represented by

$$f_{y1} = -\frac{h_o}{2k_{my}}\left(\frac{y}{b}\right)^2 - \frac{h_o}{2k_{my}}\left(\frac{y}{b}\right) + \left(\frac{2}{b} + \frac{3}{2}\frac{h_o}{k_{my}}\right) \quad (21)$$

$$f_{yn} = (b - y)^2(b + y)^n \quad \text{for} \quad n = 2, 3, 4, \ldots, N_n \quad (22)$$

and h_o is the heat transfer coefficient at the outside surface. The computation procedure remains as discussed earlier, except Eq. (21) replaces Eq. (18), and Eq. (22) replaces Eq. (19). These boundary conditions are used to simulate an actual physical problem and demonstrate the mathematical method's versatility in conducting sensitivity studies for part geometry, material properties, and optimizing the coolant flow rate. Convective boundary conditions for aircraft are dependent upon flight conditions. Modern hypersonic air vehicles operate between Mach 5 and 8 from 18.3 to 30.5 km (60,000 to 100,000 ft) in altitude. Reference 10 presents a methodology for calculating convection coefficients in high-speed flows. That methodology is utilized to calculate the convective coefficients that bound the flight envelope of interest. The boundary conditions are listed in Table 1 and thermophysical properties are in Table 2.

The quasisteady temperature solution T^* for implementation in Eq. (6) is based on an energy balance of a linear temperature profile through the global domain.[2] When $q = 0$, the quasisteady temperature T^* is simply equal to the temperature of outside air $T_{\infty,o}$. The working fluid for this example is JP-8 jet fuel.

Figure 1a is evaluated as a baseline for the heterogeneous component with homogeneous material properties in the xy plane; fiber direction is parallel to the cooling channel. The coolant velocity is considered fully developed, whereas the average velocity serves as an undefined constant through the mathematical calculations. This allows for parametric studies of temperature distributions for various average coolant velocities. The coolant flow rate sensitivity study results are evaluated. The physical problem represents a cooling problem of a hot structure, where the localized and global domains are influenced by the cooling channel. Each point in the domain is a function of the cooling flow distance z. Realistic dimensions for the skin, cooling channel diameter, and the cooling channel spacing are utilized for this calculation. In Fig. 1 the thickness of the skin ($2b$) is set for 4.14 mm (0.163 in.), the cooling channel spacing ($2a$) is set for 4.64 mm (0.183 in.), and the cooling channel diameter ($2c$) is set for 1.6 mm (0.063 in.).

Table 1 Boundary conditions during hypersonic flight conditions

Boundary condition[a]	18.3 km (60 ft) Mach = 5	24.4 km (80 ft) Mach = 8	30.5 km (100 ft) Mach = 8
q at $x = \pm a$	0	0	0
h at $y = -b$	0 (0)	0 (0)	0 (0)
h at $y = -b$	2.84 (0.5)	2.84 (0.5)	2.84 (0.5)
h at $y = b$	27.8 (4.9)	22.0 (3.88)	14.1 (2.49)
T_{air} at $y = -b$	37.8 (100)	37.8 (100)	37.8 (100)
T_{air} at $y = b$	918 (1,685)	2,495 (4,523)	2,570 (4,659)
$T_{coolant}$	37.8 (100)	37.8 (100)	37.8 (100)

[a]Units: T in °C (°F); h in W/m^2 K (Btu/h ft^2 °F).

Table 2 Cooling channel spacing

Materials	Properties	Values[a]
Carbon–carbon:	$k_{\parallel}$ to fibers	22.0 (35.0)
	$k_{\perp}$ to fibers	4.60 (2.66)
JP-8:	ρ	782.8 (48.87)
	c_p	2.356 (0.5633)
	k	0.922 (0.533)
	μ	313.1 (210.4)

Note: a, b, and c are shown in Fig. 1.
[a]Units: k in W/m K(Btu/h ft R); ρ in kg/m^3 (lbm/ft^3); c_p in kJ/kg K (Btu/lbm R); μ in N s/m^2 (lbm/ft s).

Postprocessing temperature distribution results in the global and localized domain is conducted simultaneously utilizing three-dimensional graphical postprocessing. Data are generated to demonstrate the appropriate coolant flow rate that ensures the material and coolant remain below their maximum design-allowable temperatures. Also, the maximum for the temperature gradient must be satisfied to limit the thermal expansion stress. Figure 3 presents the centerline coolant flow rate as a function of flow distance z for different average flow velocities. Each line in the figure corresponds to a mean flow velocity of the coolant. For example, the mean velocity of 1.0161 m/s (12,000 ft/h) provides an acceptable length of 2.286 m (7.5 ft); within that range, the temperature of the jet fuel is below the acceptable limit. For comparison, the operation temperature limits for jet fuels JP-8 and JP-900 are plotted in the same figure.

Instability in the solution with a small z entrance length is observed by examining the coolant centerline temperature plots. It is noted that the first eigenvalue in the Green's function solution is dominant.[2] Next, only one of the nine terms in Eq. (7) is employed to calculate the centerline temperature for the small z effects. The centerline temperature is plotted in Fig. 4. It shows no instability of the centerline coolant temperature at small z values.

Figure 5 is an overview of the temperature field in the material domain. It shows the isotherms for $u_{av} = 0.381$ m/s (4500 ft/h) at $z = 0.762$ m (2.5 ft) on the surface between $x = -a$ and $x = a$, and $y = -b$, and $y = b$. The spacing between two adjacent isotherms represents 2.78°C (or 5°F) temperature. The isotherms show large temperature gradients near the outer surface and the temperature variation near the lower surface is small.

Basis Functions for Convective Surface at $y = -b$

A thermal barrier concept could be employed to protect the internal structure of a high-speed aircraft. It would consist of a carbon/carbon external skin, an insulation layer, and internal compartment ventilation flow, to absorb and reject the heat to

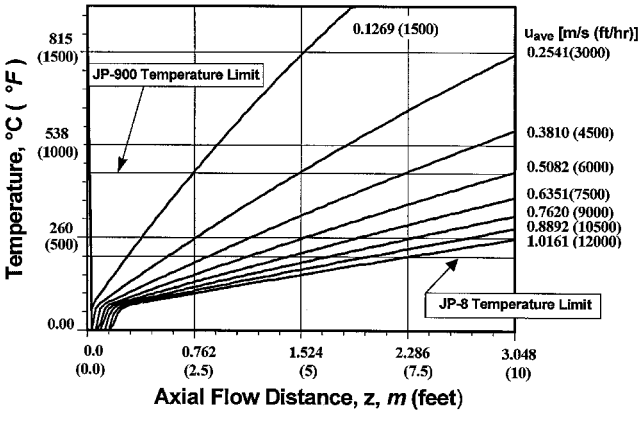

Fig. 3 Cooling channel centerline temperature.

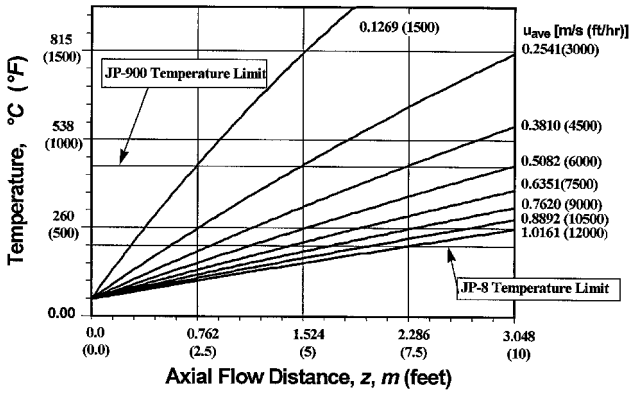

Fig. 4 Cooling channel centerline temperature, the first-term contribution.

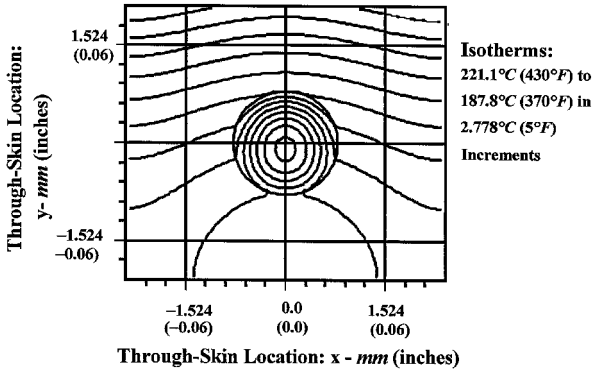

Fig. 5 Isotherms in the composite materials and in fluid.

the aircraft heat sink. The internal surface of the skin will have a 25.4 mm (1 in.) thick insulation blanket, attached to the internal surface ($y = -b$) of the skin, to protect the internal structure. The internal surface of the insulation blanket will be subject to a low convective environment. The boundary conditions would be a high-convective environment on the external surface ($y = b$) of the aircraft skin and an insulating layer followed by a low-convective environment on the internal surface ($y = -b$) of the skin. The combination of a low-convective environment and insulation on the internal surface can be expressed as the conductance or equivalent convection coefficient U, defined as

$$U = \frac{1}{(1/h_i) + (l_{\text{ins}}/k_{\text{ins}})} \tag{23}$$

where h_i is the internal convection coefficient, l_{ins} is the thickness of the insulation, and k_{ins} is the thermal conductivity of the insulation.

The y-direction basis functions for boundary conditions of the third kind on the external and internal surfaces are represented by the polynomial defined as

$$f_{y1} = \left[\gamma \left(\frac{y}{b}\right)^2 + \beta \left(\frac{y}{b}\right) + \delta\right] \tag{24}$$

Upon applying the boundary conditions of the third kind and the geometry defined in Fig. 1b. The constants are

$$\gamma = -B_2\left(-\frac{1}{b} - B_1\right) - B_1\left(-\frac{1}{b} - B_2\right) \tag{25a}$$

$$\beta = -B_2\left(-\frac{2}{b} - B_1\right) - B_1\left(\frac{2}{b} + B_2\right) \tag{25b}$$

$$\delta = \left(\frac{2}{b} + B_2\right)\left(-\frac{1}{b} - B_1\right) - \left(-\frac{2}{b} - B_1\right)\left(-\frac{1}{b} - B_2\right) \tag{25c}$$

$$B_1 = U/k_{myy} \quad \text{and} \quad B_2 = h_o/k_{myy} \tag{26}$$

$$f_{yj} = (b - y)^2(b + y)^j \quad \text{for} \quad j = 2, 3, 4, \ldots, N \tag{27}$$

and in the x direction

$$f_1 = \text{const} \tag{28a}$$

$$f_j = (a - x)^2(a + x)^j \quad \text{for} \quad j = 2, 3, 4, \ldots, N \tag{28b}$$

Auxiliary Temperature

A function T^* that makes the boundary conditions for T_z homogeneous is equal to $T_{\infty,o}$ when $q = 0$ at $y = -b$. Also, T^* is equal to $T_{\infty,o}$ when $U = h_o$ and $T_{\infty,i} = T_{\infty,o}$. However, when $T_{\infty,i} \neq T_{\infty,o}$ or $U \neq h_o$, the derivation of a functional representation of T^* requires special attention. The quasisteady temperature solution T^* for implementation of the alternative form of the Green's function, is based on a derivation of steady temperature profiles of cylinders in a global material presented by Carslaw and Jaeger.[11] For boundary conditions of the third kind, the quasisteady temperature solution in the global domain is

$$T_m^* = T_{\infty,i} + (T_{\infty,o} - T_{\infty,i})\frac{y + b + (k_{myy}/U)}{(k_{myy}/U) + 2b + (k_{myy}/h_o)} + \left(\frac{k_e - k_{myy}}{k_{myy} + k_e}\right)\left(\frac{yc^2}{x^2 + y^2}\right)\frac{(T_{\infty,o} - T_{\infty,i})}{(k_{myy}/U) + 2b + (k_{myy}/h_o)} \tag{29}$$

The quasisteady temperature solution for the localized effect of temperatures inside the cooling channel is

$$T_e^* = T_{\infty,i} + (T_{\infty,o} - T_{\infty,i})\frac{b + (k_{myy}/U)}{(k_{myy}/U) + 2b + (k_{myy}/h_o)} + \left(\frac{2yk_e}{k_{myy} + k_e}\right)\frac{(T_{\infty,o} - T_{\infty,i})}{(k_{myy}/U) + 2b + (k_{myy}/h_o)} \tag{30}$$

An examination of T_m^* and T_e^* at the cooling channel interface reveals that $T_m^* = T_e^*$ and $\partial T_m^*/\partial n = \partial T_e^*/\partial n$, thereby Eqs. (29) and (30) satisfy the continuity of T^* in the local and global domains. The temperature and heat flux can now be calculated for aircraft skins with homogeneous and orthotropic global material properties. The mathematical formulations, presented here, are applicable to domains containing more than one passage.[12] Details of the studies reported in this paper are in Ref. 13.

Results

The final example is concerned with the calculation of heat flux to the coolant within the cooling channels. Realistic parameters are used for this example. The calculations of temperature and heat flux are for the reference configuration at various flight conditions. Three flight conditions were selected: 1) Mach 5 at 18.3 km (60,000 ft), 2) Mach 8 at 24.4 km (80,000 ft), and 3) Mach 8 at 30.5 km (100,000 ft). These three flight conditions are representative of several hypersonic air-breathing propulsion systems that are being evaluated throughout the aerospace industry.

Boundary conditions are defined to simulate an actual physical problem and demonstrate the versatility of this mathematical method in conducting sensitivity studies for part geometry, material properties, and optimizing the coolant flow rate. Convective boundary conditions for aircraft are depen-

Table 3 Cooling channel spacing

Channel spacing	*a* cm (in.)	*b* cm (in.)	*c* cm (in.)
Reference	0.238 (0.0938)	0.2095 (0.0825)	0.080 (0.0315)
Four diameters	0.320 (0.126)	0.2095 (0.0825)	0.080 (0.0315)
Six diameters	0.479 (0.189)	0.2095 (0.0825)	0.080 (0.0315)
Eight diameters	0.640 (0.252)	0.2095 (0.0825)	0.080 (0.0315)
Ten diameters	0.800 (0.315)	0.2095 (0.0825)	0.080 (0.0315)

Note: *a*, *b*, and *c* are shown in Fig. 1.

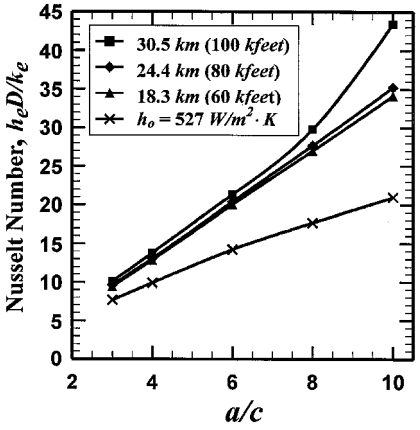

Fig. 6 Nusselt number Nu_D using homogeneous material properties.

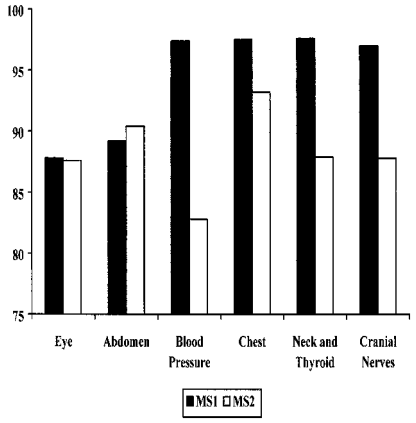

Fig. 7 Nusselt number Nu_D using orthotropic material properties.

dent upon flight conditions. Modern hypersonic air vehicles operate between Mach 5 and 8 from 18.3 to 30.5 km (60,000 to 100,000 ft) in altitude. Eckert and Drake[10] present a methodology for calculating convection coefficients in high-speed flows. Their methodology is utilized to calculate the convective coefficients that bound the flight envelope of interest. Boundary conditions are defined as in Table 1.

Several parametric studies are conducted for these flight conditions. Because this is a closed-form solution, the temperature and heat flux equations are employed to calculate fluid temperature, temperature difference between the inside and external surface, and maximum temperature on the surface, all as a function of average velocity of the fluid through the cooling channel. Temperature and heat flux data are calculated for several cooling channel spacings as listed in Table 3; these flux data are calculated for homogeneous and orthotropic global material properties. In addition, a parametric study is conducted to determine the effects of cooling channel spacing ($2a$) on the results.

For homogeneous global material properties, the alternative form of the Green's function was used to calculate the temperature and heat flux of embedded cooling channels in the carbon/carbon material. The insulation material properties were set to h_i = 2.84 W/m^2 °C (0.5 Btu/h ft^2 °F), l_{ins} = 25.4 mm (1 in.), and k_{ins} = 0.0865 W/m °C (0.05 Btu/h ft °F). The computation is repeated for orthotropic global material properties using the same parameters. The Nusselt number for the cooling channels, as defined earlier, is $Nu_D = \bar{h}_eD/k_e$.

For the reference configuration and cooling-channel spacing geometries up to 10 diameters, the Nusselt number is calculated for the boundary conditions of the third kind on the external surface and the second kind on the internal surface. A fourth condition of h_o = 567.45 W/m^2 °C (100 Btu/h ft^2 °F) is included to determine sensitivity of the Nusselt number to higher convection coefficients. Figure 6 reports the results for the homogeneous global material properties and Fig. 7 shows the results for the orthotropic global material properties. Figures 6 and 7 indicate that the Nusselt number is sensitive to cooling channel spacing and thermal conductivity; there is also a minor sensitivity to the convection coefficient. The Nusselt number for the embedded cooling channel indicates that the actual Nusselt number can differ from the theoretical values of the Nusselt number (Ref. 9) of 3.657 for constant wall temperature and 4.364 for constant wall heat flux. The Nusselt number for the reference geometry was as much as 20 times higher than the theoretical constant-wall-temperature Nusselt number.

All mathematical computation were accomplished with the symbolic mathematical software Macsyma.[14]

Remarks and Conclusions

Integral techniques were employed to study a procedure for removing heat from a hot aircraft surface by embedded cooling channels. The parametric study shows that using a constant-wall-temperature or constant-heat-flux boundary condition at the cooling channel boundary can lead to underestimation of the convection coefficient h for the cooling channel. This underestimation can result in inaccurate heat absorption calculations that can effect the design limits of aircraft skin materials or cooling fluid. Many numerical modeling codes used in the aerospace industry require the engineer to input the convection coefficient for the wall to the fluid. Without an evaluation of the Nusselt number for cases that do not have a constant-wall-temperature or a constant-heat-flux boundary condition, the engineer has to resort to these assumed boundary conditions. Thus, as demonstrated in this paper, any numerical modeling should include the contribution of energy transport in the solid wall and cooling channels.

As an important feature, this technique permits the utilization of a mathematical software package for the calculations. This goal is realistic because of the availability of powerful symbolic mathematical software packages that run on desktop personal computers. Macsyma is used to provide the symbolic computer programming capability for all of the computations needed for this mathematical methodology. Calculation of matrices A and B requires partial differential operations and dot products leading to the evaluation of integrals in Eqs. (10) and (11). Also, the eigenvalues utilizing Eq. (9) are calculated by Macsyma using the Cholesky decomposition of matrix B, performing a series of matrix operations, solving for the eigen-

values and eigenvectors, and evaluating the matrix P. For data in Fig. 2, T^* is a constant; however, in general, T^* may depend on coordinates. The alternative form of the Green's function solution, Eq. (6), may require additional differentiation and integration to calculate the auxiliary temperature: in the main domain, $T^* = T^*_m(x, y, z)$, and in the inclusion, $T^* = T^*_e(x, y, z)$. Postprocessing of the equation generated for the temperature solution is an added benefit for utilizing a symbolic mathematical software package; it permits a three-dimensional presentation of a closed-form solution. A desktop computer was used to perform all computations for simultaneously solving the heat conduction equation for a global domain and localized events.

One important feature of this method is its ability to deal effectively with contact conditions between the material domain and the fluid. It permits continuity of temperature and heat flux to be satisfied all along the tube boundaries; in contrast, many numerical techniques satisfy these conditions along isolated points. As another advantage, this Green's function solution method provides additional information as demonstrated in the postprocessing of results. Any point of interest can be evaluated without concern for grid point location. Parametric studies are possible employing this methodology and utilizing average coolant velocity and cooling channel spacing as independent constants to calculate maximum fluid temperature, maximum material temperature, and maximum temperature gradients in the composite domain. The benefits of conducting parametric studies without recalculating the entire solution is demonstrated by allowing configuration design parameters as undefined constants throughout the calculation process. This attribute can assist engineers in conducting parametric studies on temperature profiles as a function of changing design parameters.

The temperature of coolants is evaluated readily with this method. The temperature at every location in the component is available instead of just at node locations. The localized solution determines whether boiling of liquids or coking of coolants is likely to occur and a simple change in the velocity assures whether the part is cooled sufficiently and whether the design constraints of the coolant are met.

Acknowledgments

This work was partially supported by NASA/University of Texas at Arlington (UTA) Hypersonic Research Center, Grant NAGW 3714. The authors appreciate the technical assistance of D. R. Wilson, Mechanical and Aerospace Engineering Department, UTA, who provided the flight profile information.

References

[1]Anderson, D. A., Tannehill, J. C., and Pletcher, R. H., *Computational Fluid Mechanics and Heat Transfer*, Hemisphere, Washington, DC, 1964.

[2]Beck, J. V., Cole, K. D., Haji-Sheikh, A., and Litkouhi, B., *Heat Conduction Using Green's Functions*, Hemisphere, Washington, DC, 1992.

[3]Cotta, R. M., *Integral Transforms in Computational Heat and Fluid Flow*, CRC Press, Boca Raton, FL, 1993.

[4]Haji-Sheikh, A., and Lakshminarayanan, R., "Integral Solution of Diffusion Equation: Part 2—Boundary Conditions of Second and Third Kinds," *Journal of Heat Transfer*, Vol. 109, No. 3, 1987, pp. 557–562.

[5]Haji-Sheikh, A., and Beck, J. V., "Green's Function Partitioning in Galerkin-Based Solution of the Diffusion Equation," *Journal of Heat Transfer*, Vol. 112, No. 1, 1990, pp. 28–34.

[6]Kantorovich, L. V., and Krylov, V. L., *Approximate Methods of Higher Analysis*, Interscience, New York, 1958.

[7]Carnahan, B., Luther, H. A., and Wilkes, J. O., *Applied Numerical Methods*, Wiley, New York, 1969.

[8]Haji-Sheikh, A. "Heat Transfer in Heterogeneous Bodies Using Heat-Flux-Conserving Basis Functions," *Journal of Heat Transfer*, Vol. 110, No. 2, 1988, pp. 276–282.

[9]Kays, W. M., and Crawford, M. E., *Convective Heat and Mass Transfer*, 3rd ed., McGraw–Hill, New York, 1993.

[10]Eckert, E. R. G., and Drake, R. M., Jr., *Analysis of Heat and Mass Transfer*, McGraw–Hill, New York, 1972.

[11]Carslaw, H. S., and Jaeger, J. C., *Conduction of Heat in Solids*, 2nd ed., Oxford Univ. Press, Oxford, England, UK, 1959.

[12]Lee, Y.-M., and Haji-Sheikh, A., "Temperature Field in Heterogeneous Bodies: A Non-Orthogonal Solution," *Fundamentals of Conduction*, edited by M. Imber and M. M. Yovanovich, HTD-Vol. 173, American Society of Mechanical Engineers, New York, 1991, pp. 1–9.

[13]Griggs, S. C., "Temperature and Heat Flux in Embedded Cooling Channels," Ph.D. Dissertation, Univ. of Texas at Arlington, TX, Aug. 1997.

[14]Macsyma, *Mathematics and System Reference Manual*, 16th ed., Macsyma, Inc., Arlington, MA, 1996.